Geomechanics and Engineering, *Vol. 10, No. 5 (2016) 657-676*
DOI: http://dx.doi.org/10.12989/gae.2016.10.5.657

Static and seismic active lateral earth pressure coefficients for *c-ϕ* soils

Amin Keshavarz * and Zahra Pooresmaeil [a]

School of Engineering, Persian Gulf University, Bushehr, Iran

(*Received October 22, 2015, Revised February 07, 2016, Accepted February 12, 2016*)

Abstract. In this paper, the active lateral earth pressure is evaluated using the stress characteristics or slip line method. The lateral earth pressure is expressed as the lateral earth pressure coefficients due to the surcharge, the unit weight and cohesion of the backfill soil. Seismic horizontal and vertical pseudo-static coefficients are used to consider the seismic effects. The equilibrium equations along the characteristics lines are solved by the finite difference method. The slope of the ground surface, the wall angle and the adhesion and friction angle of the soil-wall interface are also considered in the analysis. A computer code is provided for the analysis. The code is capable of solving the characteristics network, determining active lateral earth pressure distribution and calculating active lateral earth pressure coefficients. Closed-form solutions are provided for the lateral earth pressure coefficients due to the surcharge and cohesion. The results of this study have a good agreement with other reported results. The effects of the geometry of the retaining wall, the soil and soil-wall interface parameters are evaluated. Non-dimensional graphs are presented for the active lateral earth pressure coefficients.

Keywords: lateral earth pressure coefficients; seismic; active; stress characteristics; slip line

1. Introduction

The stability of the retaining walls is an important issue in geotechnical engineering. It can be assessed by evaluating the lateral earth pressure in active and passive cases. Different methods are provided to assess the lateral earth pressure on the retaining walls. Some of these methods are analytical (Soubra and Macuh 2002, Shukla *et al*. 2011, Nian and Han 2012, Shukla 2012, Shukla and Bathurst 2012, Nian *et al*. 2014) and some of them are numerical (Benmeddour *et al*. 2012). Giri (Giri 2011, 2014) also used the pseudo-dynamic method to compute the distribution of the seismic earth pressure and study seismic passive earth pressure on a rigid cantilever wall.

The stress characteristics or slip line method was proposed by Sokolovskii (Sokolovskii 1960, 1965). Serrano (1972) solved the stress characteristics equations for the soil with X and Z body forces. Reece and Hettiaratchi (1989) used the stress characteristics method to estimate the passive lateral earth pressure. Using this method, Kumar and Chitikela (2002) evaluated the seismic passive lateral earth pressure. Furthermore, Cheng (2003) proposed a rotation of the axes in solving the slip line equations to assess the lateral earth pressure under the horizontal seismic

*Corresponding author, Assistant Professor, E-mail: keshavarz@pgu.ac.ir
[a] Graduate Student, E-mail: zahra.pouresmael@gmail.com

http://www.techno-press.org/?journal=gae&subpage=7 ISSN: 2005-307X (Print), 2092-6219 (Online)

loading. Peng and Chen (2013) used the slip-line method to compute the active earth pressure on retaining walls. The stress characteristics method has also been used successfully to evaluate the stability of the reinforced soil structures (Jahanandish and Keshavarz 2005, Keshavarz *et al*. 2011).

This method analyzes geotechnical problems in the stress field and assumes that the soil is associative and all points in the failure zone are in the plastic state. The distribution of the stress and failure surface shape will be determined after solving the characteristics network and this is one of the good advantages of this method.

In this paper, the stress characteristics method is used to evaluate the active lateral earth pressure on the retaining walls. The seismic effects are considered in the analysis as the horizontal and vertical pseudo-static coefficients. The lateral earth pressure coefficients are calculated using the superposition method and the results are compared with analyses without superposition. By considering the soil cohesion and the soil-wall interface adhesion, the lateral earth pressure coefficient due to the soil cohesion is also presented. The stress discontinuity is expressed and a solution is provided to modify the retaining wall problems in these special cases.

2. Theory

2.1 Equilibrium equations along the characteristics

The backfill soil is considered as a c-ϕ soil and follows the Mohr-Coulomb yield criterion, where c is the cohesion and ϕ is the friction angle. If a small element of the soil is considered in the plane strain stress field, as illustrated in Fig 1, two failure plus and minus characteristics orientations, PB and PA, can be found. The stress characteristics lines make the angle $\mu = \pi/4 - \phi/2$ with σ_1 (principal stress) axis (Sokolovskii 1965).

Each point in the soil has four features, x, z, p and ψ, where x and z are the coordinates, p is the average stress in the Mohr circle and ψ is the angle between σ_1 and the horizontal axis (Fig. 1).

As shown in Fig. 1, the angle between the stress characteristics lines is 2μ and the slope of these lines can be calculated as follows

$$\text{Plus characteristics, PB}: \quad \frac{\mathrm{d}z}{\mathrm{d}x} = \tan\left(\psi + \mu\right) \tag{1}$$

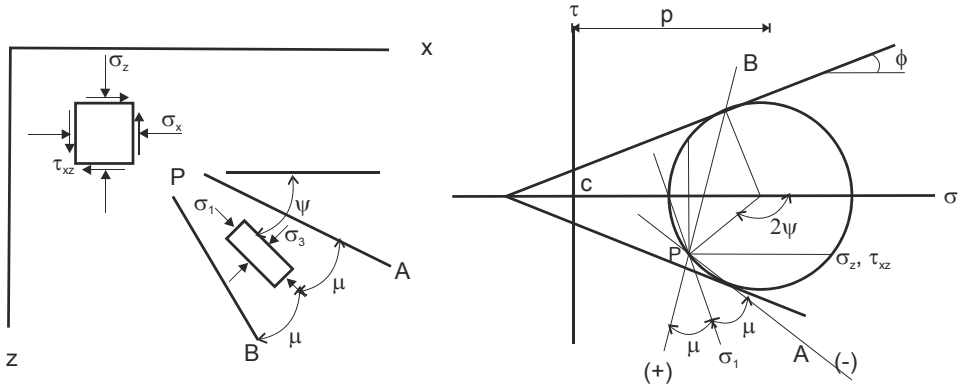

Fig. 1 Plus and minus stress characteristics orientation (σ^+,σ^-) and Mohr circle (Anvar and Ghahramani 1997)

$$\text{Minus characteristics, PA:} \quad \frac{\mathrm{d}z}{\mathrm{d}x} = \tan\left(\psi - \mu\right) \tag{2}$$

The equilibrium equations along the plus and minus characteristics can be written as (Anvar and Ghahramani 1997):

Along the plus characteristics

$$\cos\phi \mathrm{d}p + 2\left(p\sin\phi + c\cos\phi\right)\mathrm{d}\psi = \left(\cos\phi \mathrm{d}x - \sin\phi \mathrm{d}z\right)X + \left(\sin\phi \mathrm{d}x + \cos\phi \mathrm{d}z\right)Z \tag{3}$$

and along the minus characteristics

$$-\cos\phi \mathrm{d}p + 2\left(p\sin\phi + c\cos\phi\right)\mathrm{d}\psi = -\left(\cos\phi \mathrm{d}x + \sin\phi \mathrm{d}z\right)X + \left(\sin\phi \mathrm{d}x - \cos\phi \mathrm{d}z\right)Z \tag{4}$$

where X and Z are body forces along the x and z axis, respectively.

$$X = -\gamma k_h \tag{5}$$

$$Z = -\gamma\left(1 - k_v\right) \tag{6}$$

where, k_h and k_v are the horizontal and vertical pseudo-static earthquake coefficients and γ is the unit weight of the soil. If x, z, p and ψ of point A and B are known (Fig. 1), these values of any point P can be found by writing Eqs. (1) to (4) in the finite difference form

$$\begin{aligned} x_P &= \frac{x_B t_{mp} - x_A t_{mm} - z_B + z_A}{t_{mp} - t_{mm}} \\ z_P &= \left(x_P - x_B\right)t_{mm} + z_B \\ p_P &= p_B + \frac{A_2 - 2B_{mp}\left(\psi_P - \psi_B\right)}{A_{mp}} \\ \psi_P &= \frac{A_3}{A_4} \end{aligned} \tag{7}$$

The parameters in Eq. (7) are defined in Appendix 1. The trial and error procedure is used to calculate the unknown parameters (x, z, p and ψ) of point P. For a first try, it is assumed that these parameters are equal to the parameters of point A and B on the minus and plus characteristics, respectively. Then the new parameters of point P can be calculated using Eq. (7). This procedure is repeated until the difference between the new and old parameters of point P is small enough.

2.2 Boundary conditions

Fig. 2 shows the geometry of the retaining wall in active case. To solve the problem, the boundary condition along the ground surface and retaining wall will be provided in the following

2.2.1 Boundary conditions on the ground surface

In Fig. 2, β is the ground surface angle with the horizontal axis (the earth slope) and θ is the retaining wall angle with the vertical direction. The coordinates (x, z) of the point number i on the

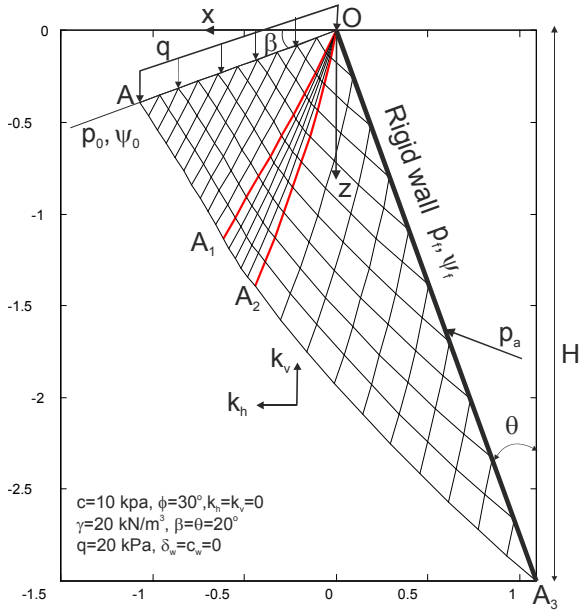

Fig. 2 Geometry of the retaining wall and a sample slip lines filed

ground surface can be calculated as

$$x_i = -\frac{L}{n}(i-1)\cos\beta, \quad z_i = x_i \tan\beta \tag{8}$$

where L is the length considered on the ground surface and n is the number of divisions. If the vertical stress q is applied on the ground surface, the normal and shear stresses for the points on the ground are

$$\begin{aligned} \sigma_0 &= q\cos\beta\left[(1-k_v)\cos\beta - k_h\sin\beta\right] \\ \tau_0 &= q\cos\beta\left[(1-k_v)\sin\beta + k_h\cos\beta\right] \end{aligned} \tag{9}$$

The Mohr circle of stress on the ground is shown in Fig. 3. The radius of Mohr circle on this boundary can be calculated as

$$R_0 = \sqrt{(\sigma_0 - p_0)^2 + \tau_0^2} = p_0\sin\phi + c\cos\phi \tag{10}$$

Therefore, the average stress on the ground (p_0) is obtained by solving Eq. (10)

$$p_0 = \frac{\sigma_0 + c\cos\phi\sin\phi - \sqrt{(\sigma_0\sin\phi + c\cos\phi)^2 - (\tau_0\cos\phi)^2}}{\cos^2\phi} \tag{11}$$

Using the Mohr circle of stress (Fig. 3), the angle ψ on the ground surface (ψ_0) can be calculated as

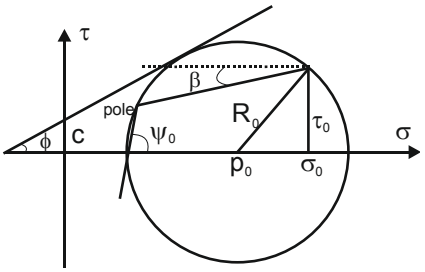

Fig. 3 Mohr circle of stress on the ground surface

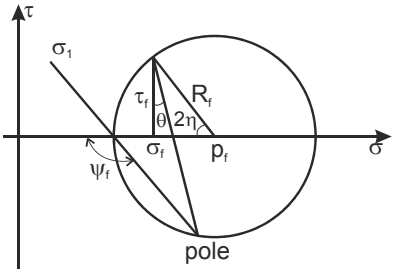

Fig. 4 Mohr circle of stress on the wall

$$\begin{aligned} &\text{if } q=0: \quad \psi_0=\beta+\frac{\pi}{2} \\ &\text{else} \qquad \psi_0=\frac{\pi}{2}+0.5\left[\beta-\delta-\sin^{-1}\left(\frac{p_0\sin(\delta+\beta)}{R_0}\right)\right] \end{aligned} \tag{12}$$

where

$$\tan\delta=\frac{k_h}{1-k_v} \tag{13}$$

2.2.2 Boundary conditions on the retaining wall

Fig. 4 shows the Mohr circle of stress on the retaining wall. Using this figure, it can be found that

$$\begin{aligned} \psi_f &= \frac{\pi}{2}+\eta+\theta \\ \sigma_f &= p_f - R_f\cos 2\eta \\ \tau_f &= c_w+\sigma_f\tan\delta_w \end{aligned} \tag{14}$$

where σ_f and τ_f are the normal and shear stress on the retaining wall, respectively. c_w and δ_w are the adhesion and friction angle in the interface between the soil and wall. The angle ψ on the wall (ψ_f) can be calculated from Eq. (14)

$$\psi_f=\frac{\pi}{2}+\theta+0.5\left[-\delta_w+\sin^{-1}\left(\frac{p_f\sin\delta_w+c_w\cos\delta_w}{R_f}\right)\right] \tag{15}$$

2.3 Analysis procedure

A computer code is provided to analyze the problem. The code can calculate the network and compute the lateral earth pressure along the retaining wall. The overall procedure is similar to the traditional stress characteristics or slip line method. Calculation starts from the ground surface (Boundary OA, Fig. 2). Knowing the x, z, p and ψ at the boundary OA, the network in the Rankin zone OAA_1 can be obtained using the Eq. (7). Since the p and ψ in the left and right of point O is different, a singularity exists at this point.

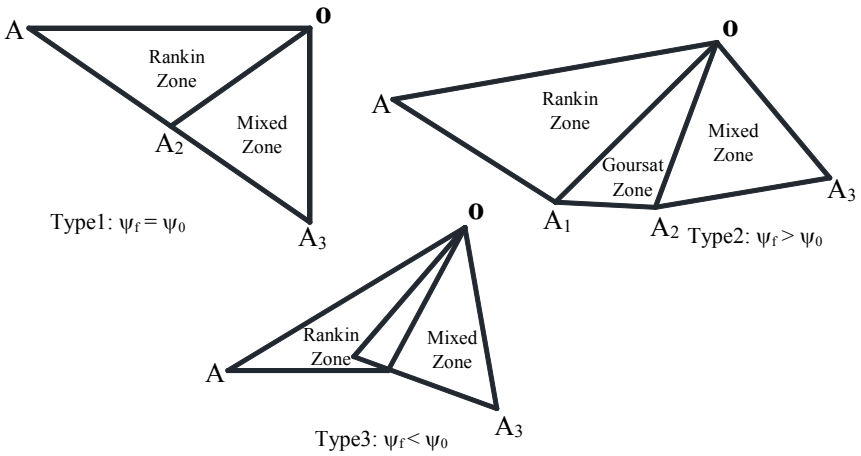

Fig. 5 Different types of the retaining wall problem

At point O, dx = dz = 0, and p can be determined from Eq. (3) as

$$p = -c\cot\phi + (p_0 + c\cot\phi)\exp\left[-2\tan\phi\left(\psi - \psi_0\right)\right] \tag{16}$$

There are three different types of problems according to the values of ψ_0 and ψ_f. These problems have been shown in Fig. 5.

Type 1, $\psi_f = \psi_0$:

If $\psi_f = \psi_0$, the Goursat zone will be removed and the characteristics network includes Rankin and Mixed zone. In this case, after solving the Rankin zone, the network in the mixed zone can be determined knowing the information on line OA_2 and the boundary conditions on the wall.

Type 2, $\psi_f > \psi_0$:

If $\psi_f > \psi_0$, the characteristics network includes three zones: Rankin, Goursat and mixed. In this case after solving the Rankin zone, the Goursat zone must be determined. The Goursat zone can be solved using the information at point O and line OA_1. The mixed zone is obtained similar to type 1 problem.

Type 3, $\psi_f < \psi_0$:

If $\psi_f < \psi_0$, the Goursat zone will be removed similar to type 1 and the Rankin and mixed zone will be wrapped. A stress discontinuity happens in this case. An algorithm proposed by Lee and Herington (1972) is modified to solve the stress discontinuity. This algorithm proposes a solution to solve the retaining wall problem in such cases and is explained in the following section.

2.4 Stress discontinuity

As mentioned, if the angle ψ on the wall is lower than the angle ψ on the ground surface ($\psi_f < \psi_0$), the stress discontinuity happens in the stress field. In order to solve the discontinuity, an element of the soil is considered on the discontinuity line (see Fig. 6). The Mohr circle is shown according to the soil element on the discontinuity line.

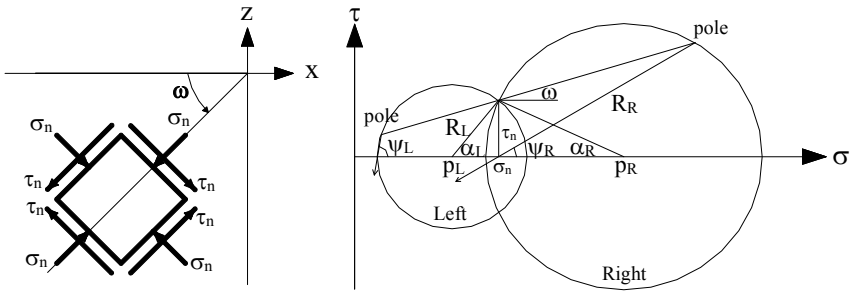

Fig. 6 The soil element on the stress discontinuity line and Mohr circle

According to the Mohr circle shown in Fig. 6, the following relations can be written

$$\begin{aligned} R_R \sin 2(\psi_R - \omega) &= R_L \sin 2(\psi_L - \omega) \\ p_R - R_R \cos 2(\psi_R - \omega) &= p_L - R_L \cos 2(\psi_L - \omega) \end{aligned} \tag{17}$$

where, ω is the direction of the discontinuity line, p_R, R_R and ψ_R are the average stress p, the radius of Mohr circle and the angle ψ related to the right side of the discontinuity line, respectively. p_L, R_L and ψ_L are the similar variables for the left side of the discontinuity line.

The direction of the discontinuity line can be calculated from Eq. (17) as

$$\omega = 0.5\left[\psi_R + \psi_L - \cos^{-1}\left(\sin\phi\cos(\psi_R - \psi_L)\right)\right] \tag{18}$$

If ω, R_L and ψ_L are known, R_R and ψ_R can be obtained from Eq. (17) as

$$\begin{aligned} \psi_R &= \tan^{-1}\left(\frac{\cos(\psi_L - 2\omega) - \sin\phi\cos\psi_L}{\sin(\psi_L - 2\omega) - \sin\phi\sin\psi_L}\right) \\ p_R &= \frac{R_L \sin 2(\psi_L - \omega)}{\sin\phi \sin 2(\psi_R - \omega)} - c\cot\phi \end{aligned} \tag{19}$$

Knowing the left-sided characteristics of the singularity point O (the values on the ground) and from Eq. (18), the first direction (ω_0) is obtained and the intersection between the discontinuity line and the characteristics network (point G in Fig. 7(a)) is calculated. The coordinates of the point G can be obtained from the intersection of the lines OG and EF.

$$\begin{aligned} x_G &= \frac{x_o \tan\omega_0 + z_E - z_o - m_2 x_E}{\tan\omega_0 - m_2} \\ z_G &= z_o + \tan\omega_0 (x_G - x_o) \end{aligned} \tag{20}$$

where $m_2 = (z_F - z_E)/(x_F - x_E)$. Now, the values p_G and ψ_G at the left side of the point G can be calculated using linear interpolation

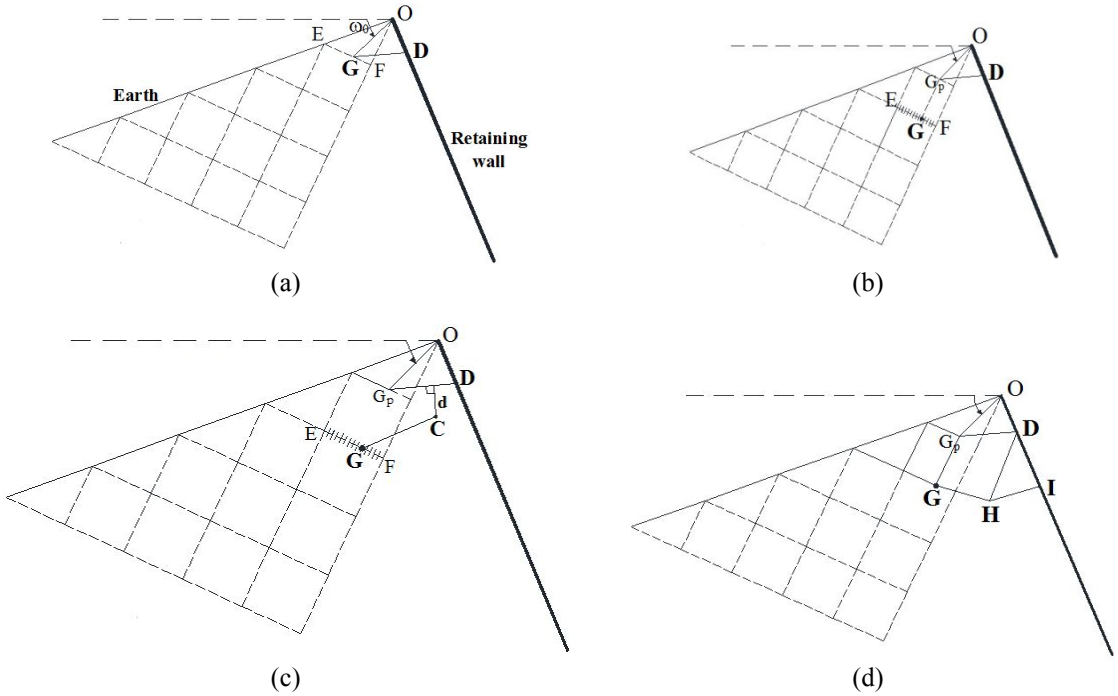

Fig. 7 The algorithm for solving the stress discontinuity

$$p_{GL} = p_E + \left(p_F - p_E\right)\frac{\mathrm{EG}}{\mathrm{EF}}$$
$$\psi_{GL} = \psi_E + \left(\psi_F - \psi_E\right)\frac{\mathrm{EG}}{\mathrm{EF}} \tag{21}$$

where

$$\mathrm{EG} = \sqrt{\left(x_G - x_E\right)^2 + \left(z_G - z_E\right)^2}$$
$$\mathrm{EF} = \sqrt{\left(x_G - x_F\right)^2 + \left(z_G - z_F\right)^2} \tag{22}$$

Knowing ω_0, p_{GL} and ψ_{GL}, the stress p and the angle ψ at the right side of the point G are obtained using Eq. (19). Then, the point on the wall (the point D in Fig. 7(b)) is calculated using Eq. (4) in the finite difference form.

Now, the next step should be solved. A line with the angle ω_p (or ω_0 in this step) is drawn from the point G_p (the previous point G as shown in Fig. 7(c) and Fig. 7(d)). The segment of the characteristics network that encounters with the line is determined (line EF in Fig. 7(b)). This segment is divided into n_G parts. The information of these n_G points is calculated with the interpolation between points E and F. For each of these n_G points (like G in Fig. 7(c)), the p and at the right side can be calculated from Eq. (19). Assuming that GC and G_pC are the minus and plus characteristics lines, the x, z, p and ψ of point C can be obtained (see Fig. 7(c)). The distance between point C and line G_pD (d in Fig. 7(c)) is calculated. Within these n_G points, the point that has the minimum distance d, is selected as the exact point G.

Knowing the information in the right side of G, the points H and I can be obtained (Fig. 7(d)). This procedure is repeated to solve the whole network.

3. Results

After solving the network, the normal (σ_f) and shear (τ_f) stress distribution along the retaining wall are obtained. Integrating these stresses along the wall, the active lateral earth pressure can be obtained.

The active lateral earth force can be written as (Chen and Liu 1990)

$$p_a = \frac{1}{2}\gamma H^2 k_{a\gamma} + qHk_{aq} - cHk_{ac} \tag{23}$$

where H is the height of the retaining wall. $k_{a\gamma}$, k_{aq} and k_{ac}, are the active lateral earth pressure coefficients due to the unit weight of the soil, surcharge and cohesion, respectively.

To calculate the lateral earth pressure coefficients, the superposition principle is used. In order to calculate $k_{a\gamma}$, the cohesion of the soil and surcharge should be assumed as zero. If the surcharge and cohesion are equal to zero, the problem cannot be solved for the singularity point, therefore, a small amount of the surcharge (q = 0.01 kPa) is assumed. The unit weight of the soil is assumed to be 18 kN/m^3 in all calculations. To increase accuracy and remove the surcharge effect, $k_{a\gamma}$ is written as

$$k_{a\gamma} = k'_{a\gamma} - \frac{2qk_{aq}}{\gamma H} \tag{24}$$

where, $k_{a\gamma}$ is the exact value of the lateral earth pressure coefficient where the surcharge effect is removed and $k'_{a\gamma}$ is the lateral earth pressure coefficient obtained from analyzing the retaining wall with q = 0.01 kPa.

The unit weight and cohesion of the soil are considered zero to calculate k_{aq}. Also, the unit weight of the soil and surcharge have the zero values in obtaining k_{ac}. For k_{aq} and k_{ac}, the stress distribution on the wall is uniform. A closed-form solution can be found for k_{aq} and k_{ac}

$$k_{aq} = A_q \frac{1+\sin(\phi)\cos 2\left(\theta-\psi_f\right)}{\cos\theta\cos\delta_w} \tag{25}$$

$$k_{ac} = \frac{\sqrt{A_c{}^2 + \left(A_c\sin\phi+\cos\phi\right)^2 + 2A_c\left(A_c\sin\phi+\cos\phi\right)\cos 2\left(\theta-\psi_f\right)}}{\cos\theta} \tag{26}$$

The derivations of these equations and their parameters are explained in Appendix 2. For k_{ac} a nonlinear equation for ψ_f must be solved first (see Appendix 2).

Table 1 shows the static lateral earth pressure coefficients due to the unit weight of the soil. In this table, the stress characteristics method is compared with the limit equilibrium and limit analysis methods (Chen 1975). The results show that the calculated $k_{a\gamma}$ of this study are very close to other results for smooth walls. However, for the rough wall (i.e., $\delta_w \neq 0$), the error between this

study and other methods increases, as the friction angle of the wall increases.

In order to study the effects of the friction angle of the soil and the wall, the stability analyses are done in different conditions. Some results are shown in Table 2. As seen, the results of this study are very close to those of numerical solution of Benmeddour *et al*. (2012) and analytical solution of Soubra and Macuh (2002) and in some cases are the same.

The effects of ϕ and δ_w on static $k_{a\gamma}$ for $\beta = \theta = 0$ are shown in Fig. 8. It is clear that an increase in the friction angle of the soil decreases the active lateral earth pressure coefficient. Also, $k_{a\gamma}$ decreases in some cases and increases in other cases by increasing δ_w.

Table 1 Static $k_{a\gamma}$ and a comparison between different methods

ϕ (degree)	δ_w (degree)	β (degree)	Present study	Limit equilibrium (Chen 1975)	Limit analysis (Chen 1975)
20	0	0	0.490	0.490	0.490
	0	10	0.574	0.569	0.566
	10	0	0.449	0.426	0.446
	10	10	0.531	0.507	0.531
	20	0	0.440	0.350	0.426
	20	10	0.524	0.430	0.516
30	0	0	0.333	0.333	0.333
	0	10	0.375	0.374	0.372
	0	20	0.450	0.441	0.439
	10	0	0.309	0.290	0.307
	10	10	0.349	0.334	0.35
	10	20	0.422	0.401	0.42
	20	0	0.301	0.247	0.297
	20	10	0.341	0.282	0.338
	20	20	0.414	0.334	0.413

Table 2 The effect of the friction angle of the soil and wall on the static lateral earth pressure coefficient $k_{a\gamma}$

	$k_{a\gamma}$ for smooth wall ($\delta_w = 0$)						$k_{a\gamma}$ for rough wall ($\delta_w / \phi = 1/3$)					
	$\phi = 30°$			$\phi = 35°$			$\phi = 30°$			$\phi = 35°$		
β / ϕ	Present study	Benmeddour *et al*. (2012)	Soubra and Macuh (2002)	Present study	Benmeddour *et al*. (2012)	Soubra and Macuh (2002)	Present study	Benmeddour *et al*. (2012)	Soubra and Macuh (2002)	Present study	Benmeddour *et al*. (2012)	Soubra and Macuh (2002)
0	0.333	0.330	0.333	0.271	0.271	0.271	0.309	0.308	0.309	0.252	0.247	0.251
-1/3	0.375	0.373	0.374	0.307	0.295	0.306	0.349	0.349	0.350	0.286	0.287	0.286
-1/2	0.405	0.407	0.402	0.333	0.320	0.330	0.379	0.387	0.379	0.312	0.309	0.311
-2/3	0.450	0.440	0.441	0.372	0.355	0.365	0.475	0.415	0.420	0.349	0.335	0.347

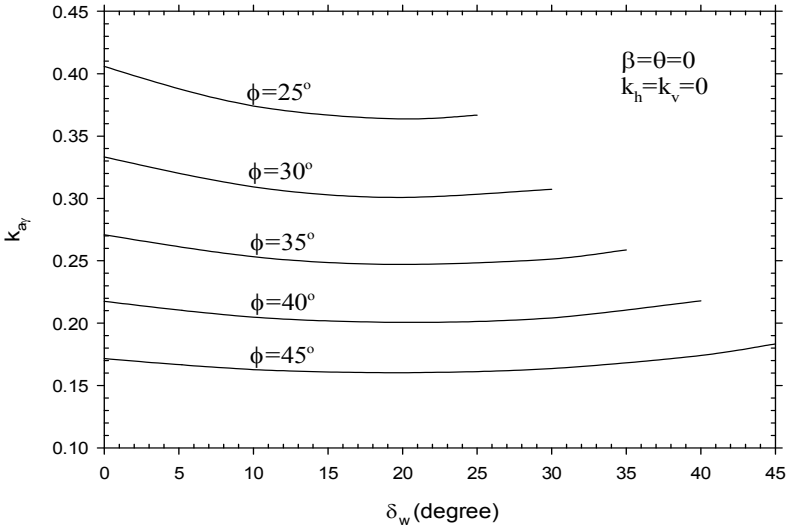

Fig. 8 Static lateral earth pressure coefficient $k_{a\gamma}$ for the vertical wall and the horizontal earth

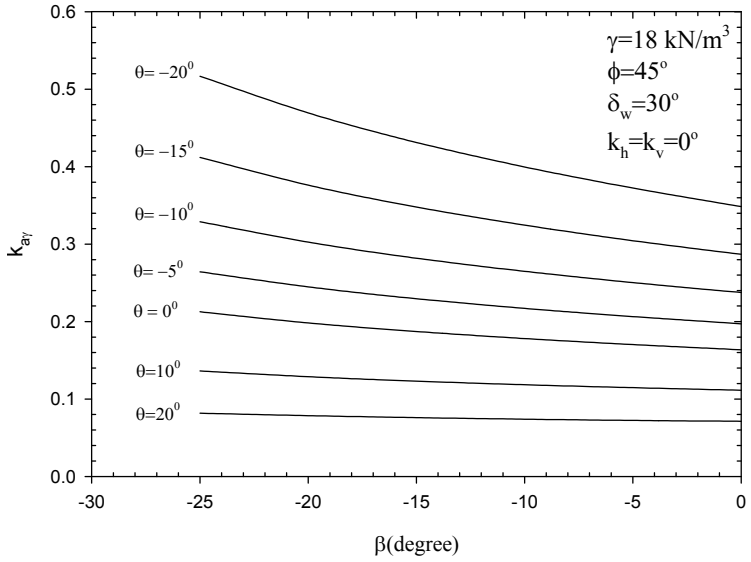

Fig. 9 Impact of the earth slope and wall angle on the static lateral earth pressure coefficient $k_{a\gamma}$

In Fig. 9 the effect of the earth slope β and wall angle θ is considered for ϕ = 45° and δ_w=30°. The results show a decrease of $k_{a\gamma}$ with an increase of β or θ. The effect of β on the $k_{a\gamma}$ values is insignificant for positive values of θ. Fig. 10 and 11 illustrate the lateral earth pressure coefficients for the wall with different angles. The results show that both $k_{a\gamma}$ and k_{aq} decrease with increase in θ and β.

As mentioned before, the dynamic effects are considered as the horizontal and vertical pseudo-static coefficients. The effects of k_h on $k_{a\gamma}$ and k_{aq} are shown in Figs. 12 and 13, respectively. As

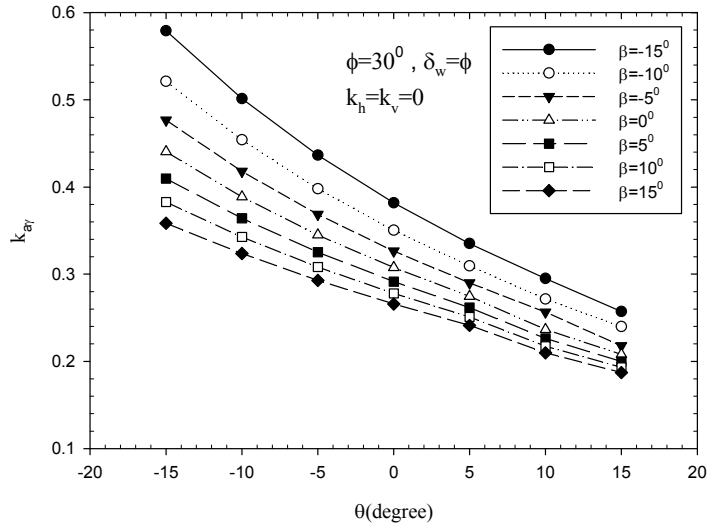

Fig. 10 Lateral earth pressure coefficient $k_{a\gamma}$ for differnet wall angles and earth slopes

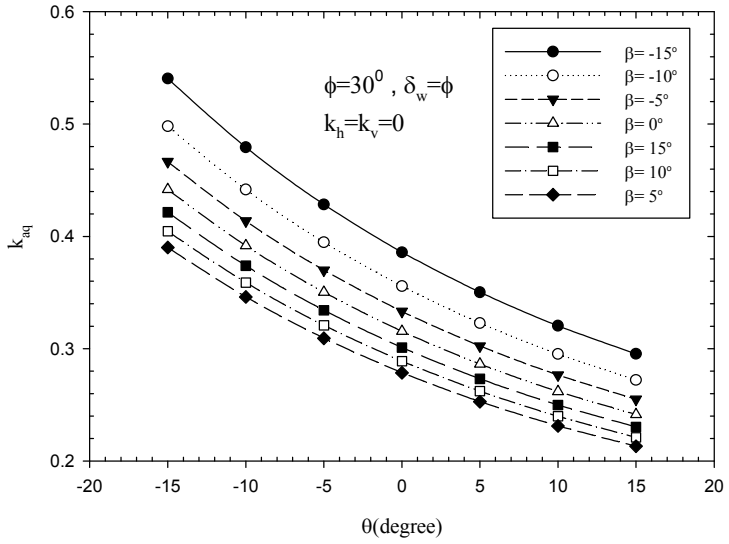

Fig. 11 Lateral earth pressure coefficient k_{aq} for different wall angles and earth slopes

shown, the horizontal and vertical earthquake coefficients have a considerable effect on the lateral earth pressure coefficients $k_{a\gamma}$ and k_{aq}. An increase in the horizontal earthquake coefficient increases the $k_{a\gamma}$ and k_{aq} values.

The effect of the horizontal and vertical earthquake coefficients on $k_{a\gamma}$ is also shown in Table 3. The results show that increasing the vertical earthquake coefficient increases the lateral earth pressure coefficient. The $k_{a\gamma}$ values have considerable increase in presence of both horizontal and vertical earthquake coefficients.

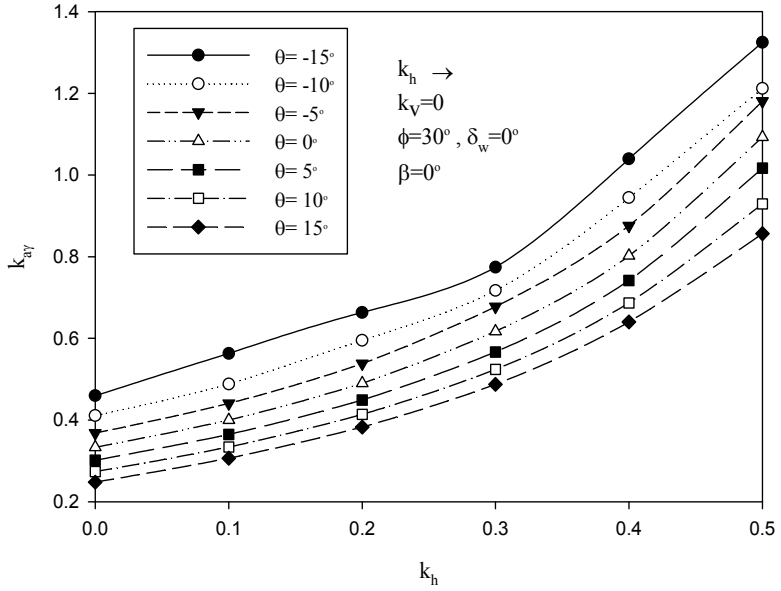

Fig. 12 The effect of horizontal earthquake coefficient on the lateral earth pressure coefficient $k_{a\gamma}$

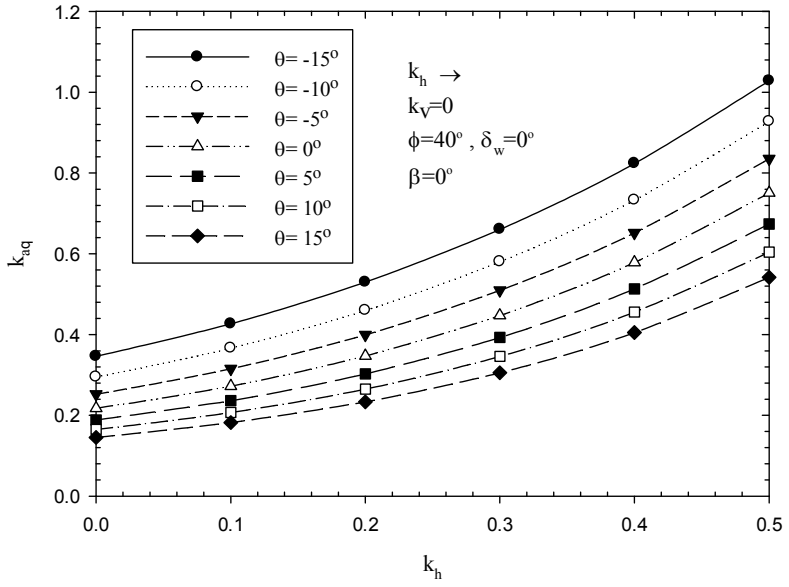

Fig. 13 The effect of horizontal earthquake coefficient on the lateral earth pressure coefficient k_{aq}

Table 4 shows the results of the lateral earth pressure coefficient due to the soil cohesion, k_{ac}, for different cases. The effect of the soil-wall interface adhesion c_w on k_{ac} is also considered in the analyses. It is clear that considering the parameter c_w increases k_{ac}. As shown in Table 4, increasing the friction angle of the soil and the earth slope (β), decreases the k_{ac} values and increasing the wall angle (θ) causes an increase in k_{ac}. It is worth mentioning that increasing δ_w increases k_{ac} in

Table 3 The effect of the horizontal and vertical earthquake coefficients on the lateral earth pressure coefficient $k_{a\gamma}$

		$k_{a\gamma}$ for $\phi = 40°$		
	δ_w / ϕ	$k_h = 0.0$ $k_v = 0.0$	$k_h = 0.1\rightarrow$ $k_v = 0.0$	$k_h = 0.1\rightarrow$ $k_v = 0.1\downarrow$
$\theta = 0$, $\beta = -30°$	0	0.327	0.501	0.523
	0.5	0.307	0.477	0.500
	1	0.340	0.540	0.565
$\theta = 0$, $\beta = 30°$	0	0.176	0.208	0.226
	0.5	0.161	0.192	0.208
	1	0.173	0.208	0.225
$\theta = 0$, $\beta = 0°$	0	0.217	0.271	0.292
	0.5	0.201	0.253	0.268
	1	0.218	0.279	0.299

Table 4 Lateral earth pressure coefficients k_{ac} for different values of θ, β, ϕ, δ_w/ϕ and c_w/c

		$\beta = -30°$						$\beta = 0°$					
		$c_w/c = 0$			$c_w/c = \tan\delta_w/\tan\varphi$			$c_w/c = 0$			$c_w/c = \tan\delta_w/\tan\varphi$		
θ	ϕ	$\delta_w/\phi = 0$	$\delta_w/\phi = 0.5$	$\delta_w/\phi = 1$	$\delta_w/\phi = 0$	$\delta_w/\phi = 0.5$	$\delta_w/\phi = 1$	$\delta_w/\phi = 0$	$\delta_w/\phi = 0.5$	$\delta_w/\phi = 1$	$\delta_w/\phi = 0$	$\delta_w/\phi = 0.5$	$\delta_w/\phi = 1$
-30	0	2.309	2.309	2.309	2.309	2.309	2.309	2.309	2.309	2.309	2.309	2.309	2.309
	10	1.938	1.802	1.680	1.938	2.229	2.435	1.050	0.989	0.938	1.050	1.399	1.714
	20	1.617	1.436	1.294	1.617	1.780	1.898	0.939	0.857	0.802	0.939	1.176	1.408
	30	1.333	1.158	1.046	1.333	1.420	1.488	0.822	0.745	0.714	0.822	0.979	1.155
	40	1.077	0.936	0.877	1.077	1.120	1.157	0.699	0.645	0.655	0.699	0.800	0.938
-15	0	2.613	2.613	2.613	2.613	2.613	2.613	2.613	2.613	2.613	2.613	2.613	2.613
	10	2.102	1.951	1.808	2.102	2.334	2.489	1.342	1.254	1.356	1.342	1.635	1.862
	20	1.692	1.491	1.320	1.692	1.809	1.888	1.161	1.043	1.064	1.161	1.342	1.490
	30	1.351	1.155	1.011	1.351	1.407	1.446	0.988	0.875	0.875	0.988	1.096	1.193
	40	1.061	0.897	0.805	1.061	1.085	1.103	0.821	0.733	0.745	0.821	0.882	0.946
0	0	3.047	3.047	3.047	3.047	3.047	3.047	3.047	3.047	3.047	3.047	3.047	3.047
	10	2.351	2.177	2.006	2.351	2.552	2.680	1.678	1.560	1.455	1.678	1.930	2.109
	20	1.827	1.595	1.383	1.827	1.919	1.977	1.400	1.244	1.121	1.400	1.541	1.644
	30	1.417	1.186	1.000	1.417	1.455	1.481	1.155	1.003	0.906	1.155	1.230	1.288
	40	1.084	0.885	0.753	1.084	1.099	1.109	0.933	0.810	0.759	0.933	0.970	1.002

Table 4 Lateral earth pressure coefficients k_{ac} for different values of θ, β, ϕ, δ_w/ϕ and c_w/c

θ	ϕ	$\beta = -30°$						$\beta = 0°$					
		$c_w/c = 0$			$c_w/c = \tan\delta_w/\tan\varphi$			$c_w/c = 0$			$c_w/c = \tan\delta_w/\tan\varphi$		
		$\delta_w/\phi = 0$	$\delta_w/\phi = 0.5$	$\delta_w/\phi = 1$	$\delta_w/\phi = 0$	$\delta_w/\phi = 0.5$	$\delta_w/\phi = 1$	$\delta_w/\phi = 0$	$\delta_w/\phi = 0.5$	$\delta_w/\phi = 1$	$\delta_w/\phi = 0$	$\delta_w/\phi = 0.5$	$\delta_w/\phi = 1$
15	0	3.697	3.697	3.697	3.697	3.697	3.697	3.697	3.697	3.697	3.697	3.697	3.697
	10	2.738	2.528	2.313	2.738	2.924	3.039	2.102	1.951	1.808	2.102	2.334	2.489
	20	2.057	1.776	1.497	2.057	2.134	2.181	1.692	1.491	1.320	1.692	1.809	1.888
	30	1.552	1.263	1.011	1.552	1.581	1.599	1.351	1.155	1.011	1.351	1.407	1.446
	40	1.162	0.901	0.713	1.162	1.171	1.178	1.061	0.897	0.805	1.061	1.085	1.103
30	0	4.728	4.728	4.728	4.728	4.728	4.728	3.519	3.519	3.519	3.519	3.519	3.519
	10	3.362	3.096	2.808	3.362	3.550	3.661	2.715	2.514	2.316	2.715	2.947	3.094
	20	2.447	2.081	1.686	2.447	2.517	2.558	2.110	1.842	1.597	2.110	2.216	2.283
	30	1.801	1.409	1.040	1.801	1.825	1.839	1.636	1.369	1.155	1.636	1.681	1.710
	40	1.325	1.349	1.668	1.325	1.269	1.336	1.252	1.021	0.869	1.252	1.331	1.281

Table 5 The superposition effects on the results of the analysis ($c/(\gamma H) = 0.1$, $\phi = 30^o$, $k_h = k_v = 0$, $c_w = 0$)

δ_w	$k_{a\gamma}$	k_{aq}	k_{ac}	$q = 0$			$q = 20$ kPa		
				$\frac{p_a}{\gamma H^2}$ superposition, Eq. (23)	$\frac{p_a}{\gamma H^2}$ without superposition, computer code	Error (%)	$\frac{p_a}{\gamma H^2}$ superposition, Eq. (23)	$\frac{p_a}{\gamma H^2}$ without superposition, computer code	Error (%)
0	0.333	0.333	1.155	0.051	0.051	0	0.175	0.175	0
10	0.305	0.314	1.048	0.048	0.048	0	0.164	0.162	1
20	0.283	0.313	0.965	0.045	0.046	3	0.161	0.156	3
30	0.266	0.342	0.908	0.042	0.047	9	0.169	0.156	7

some cases and causes a decrease in other cases.

As stated before, in this paper the principle of superposition is used to evaluate the lateral earth pressure coefficients. Table 5 shows the superposition effect on the results. As seen, in this example, the errors in considering the superposition are small and in some cases are zero.

4. Conclusions

In this paper, the active lateral earth pressure was calculated using the stress characteristics or the slip line method. The total lateral earth force was presented as the lateral earth pressure coefficients due to the unit weight ($k_{a\gamma}$), surcharge (k_{aq}) and cohesion (k_{ac}). The seismic effects

were considered as the horizontal and vertical pseudo-static earthquake coefficients. Based on the theory of stress characteristics method, a computer code was written, which can be used to calculate the active lateral earth pressure in c-ϕ soil behind the rigid retaining walls and to compute the failure zone. Closed form solutions were provided for k_{aq} and k_{ac}.

Using the computer code, the active lateral earth pressure coefficients were calculated, the results were compared with other methods and the effects of different parameters on the active lateral earth pressure coefficients were considered. The results show that the stress characteristics method has good capability in calculating the lateral earth pressure coefficients in static and seismic cases.

The results of this method is very close to the limit equilibrium and limit analysis methods for the smooth wall and the error increases as the friction angle of the wall increases.

The effects of different parameters on the active lateral earth pressure coefficients are, increasing in any of the parameters ϕ, the earth slope and the wall angle decreases $k_{a\gamma}$ and k_{aq} and increasing the horizontal and vertical earthquake coefficient causes an increase in $k_{a\gamma}$ and k_{aq}. Also, the active lateral earth pressure coefficients due to the unit weight of the soil and surcharge increase in some cases and decrease in other cases, as the friction angle of the wall increases. The effects of the friction angle of the soil, the friction angle of the wall and the earth slope are the same for the active lateral earth pressure coefficient due to the cohesion.

References

Anvar, S. and Ghahramani, A. (1997), "Equilibrium equations on zero extension lines and its application to soil engineering", *Iran. J. Sci. Technol.*, **21**(1), 11-34.

Benmeddour, D., Mellas, M., Frank, R. and Mabrouki, A. (2012), "Numerical study of passive and active earth pressures of sands", *Comput. Geotech.*, **40**, 34-44.

Chen, W.F. (1975), *Limit Analysis and Soil Plasticity*, Elsevier.

Chen, W. and Liu, X. (1990), *Limit Analysis in Soil Mechanics*, Elsevier.

Cheng, Y. (2003), "Seismic lateral earth pressure coefficients for *c–f* soils by slip line method", *Comput. Geotech.*, **30**(8), 661-670.

Giri, D. (2011), "Pseudo-dynamic approach of seismic earth pressure behind cantilever retaining wall with inclined backfill surface", *Geomech. Eng., Int. J.*, **3**(4), 255-266.

Giri, D. (2014), "Pseudo-dynamic methods for seismic passive earth pressure behind a cantilever retaining wall with inclined backfill", *Geomech. Geoeng.*, **9**(1), 72-78.

Jahanandish, M. and Keshavarz, A. (2005), "Seismic bearing capacity of foundations on reinforced soil slopes", *Geotext. Geomembr.*, **23**(1), 1-25.

Keshavarz, A., Jahanandish, M. and Ghahramani, A. (2011), "Seismic bearing capacity analysis of reinforced soils by the method of stress characteristics", *Iran. J. Sci. Technol., Transact. B-Eng.*, **35**(C2), 185-197.

Kumar, J. and Chitikela, S. (2002), "Seismic passive earth pressure coefficients using the method of characteristics", *Can. Geotech. J.*, **39**(2), 463-471.

Lee, I. and Herington, J. (1972), "A theoretical study of the pressures acting on a rigid wall by a sloping earth or rock fill", *Geotechnique*, **22**(1), 1-26.

Nian, T. and Han, J. (2012), "Analytical solution for Rankine's seismic active earth pressure in c-ϕ soil with infinite slope", *J. Geotech. Geoenviron. Eng.*, **139**(9), 1611-1616.

Nian, T.K., Liu, B., Han, J. and Huang, R.Q. (2014), "Effect of seismic acceleration directions on dynamic earth pressures in retaining structures", *Geomech. Eng., Int. J.*, **7**(3), 263-277.

Peng, M.X. and Chen, J. (2013), "Slip-line solution to active earth pressure on retaining walls",

Geotechnique, **63**(12), 1008-1019.
Reece, A. and Hettiaratchi, D. (1989), "A slip-line method for estimating passive earth pressure", *J. Agric. Eng. Res.*, **42**(1), 27-41.
Serrano, A. (1972), "The method of associated fields of stress and velocity and its application to earth pressure problems", *Proceedings of the 5th European Conference on Soil Mechanics and Foundation Engineering*, Madrid, Spain, April.
Shukla, S. (2012), "An analytical expression for the seismic passive earth pressure from the c-f soil backfills on rigid retaining walls with wall friction and adhesion", *Int. J. Geotech. Eng.*, **6**(3), 365-370.
Shukla, S.K. and Bathurst, R.J. (2012), "An analytical expression for the dynamic active thrust from c-f soil backfill on retaining walls with wall friction and adhesion", *Geomech. Eng., Int. J.*, **4**(3), 209-218.
Shukla, S., Sivakugan, N. and Das, B. (2011), "Analytical expression for dynamic passive pressure from *c-f* soil backfill with surcharge", *Int. J. Geotech. Eng.*, **5**(3), 357-362.
Sokolovskii, V.V. (1960), *Statics of Soil Media*, Butterworths Scientific Publications.
Sokolovskii, V.V.e. (1965), *Statics of Granular Media*, Pergamon Press.
Soubra, A.H. and Macuh, B. (2002), "Active and passive earth pressure coefficients by a kinematical approach", *Proceedings of the ICE-Geotechnical Engineering*, **155**(2), 119-131.

CC

Appendix 1

The parameters in Eq. (7) can be calculated as

$$t_{mp} = \frac{\tan\left(\psi_C + \mu_C\right) + \tan\left(\psi_B + \mu_B\right)}{2}$$
$$t_{mm} = \frac{\tan\left(\psi_C - \mu_C\right) + \tan\left(\psi_A - \mu_A\right)}{2} \tag{27}$$

$$A_3 = \left[p_B - p_A + \frac{A_2 + 2B_{mp}\psi_B}{A_{mp}} \right] A_{mm} - 2B_{mm}\psi_A - A_1$$
$$A_4 = 2\left(\frac{A_{mm}B_{mp}}{A_{mp}} - B_{mm} \right) \tag{28}$$

$$A_{mm} = -\frac{\cos\phi_P + \cos\phi_A}{2}$$
$$B_{mm} = \frac{p_P \sin\phi_P + c_P \cos\phi_P + p_A \sin\phi_A + c_A \cos\phi_A}{2}$$
$$C_{mm} = -\left[\frac{\cos\phi_P + \cos\phi_A}{2}\left(x_P - x_A\right) + \frac{\sin\phi_P + \sin\phi_A}{2}\left(z_P - z_A\right) \right] X \tag{29}$$
$$D_{mm} = \left[\frac{\sin\phi_P + \sin\phi_A}{2}\left(x_P - x_A\right) - \frac{\cos\phi_P + \cos\phi_A}{2}\left(z_P - z_A\right) \right] Z$$
$$A_1 = C_{mm} + D_{mm}$$

$$
\begin{aligned}
A_{mp} &= \frac{\cos\phi_P + \cos\phi_B}{2} \\
B_{mp} &= \frac{p_P \sin\phi_P + c_P \cos\phi_P + p_B \sin\phi_B + c_B \cos\phi_B}{2} \\
C_{mp} &= \left[\frac{\cos\phi_P + \cos\phi_B}{2}\left(x_P - x_B\right) - \frac{\sin\phi_P + \sin\phi_B}{2}\left(z_P - z_B\right) \right] X \\
D_{mp} &= \left[\frac{\sin\phi_P + \sin\phi_B}{2}\left(x_P - x_B\right) + \frac{\cos\phi_P + \cos\phi_B}{2}\left(z_P - z_B\right) \right] Z \\
A_2 &= C_{mp} + D_{mp}
\end{aligned}
\tag{30}
$$

Appendix 2 – Closed form solutions for k_{ac} and k_{aq}

If the unit weight of the soil is zero, the pressure behind the wall is uniform and closed form solutions can be found for k_{ac} and k_{aq} using the Eq. (16) or Eq. (19) and the boundary conditions.

Solution for k_{aq}

If $\gamma = c = c_w = 0$ then form Eq. (23)

$$
k_{aq} = \frac{p_a}{qH} = \frac{\sqrt{{\sigma_f}^2 + {\tau_f}^2}}{q\cos\theta} \tag{31}
$$

σ_f and τ_f can be found from Eq. (14) as

$$
\begin{aligned}
\sigma_f &= p_f\left(1 + \sin\phi\cos 2\left(\theta - \psi_f\right)\right) \\
\tau_f &= \sigma_f \tan\delta_w
\end{aligned}
\tag{32}
$$

In this case, ψ_f can be simplified as

$$
\psi_f = \frac{\pi}{2} + \theta + 0.5\left[-\delta_w + \sin^{-1}\left(\frac{\sin\delta_w}{\sin\phi}\right)\right] \tag{33}
$$

The boundary conditions on the ground surface from Eqs. (11) and (12) can be written as

$$
p_0 = \frac{\sigma_0 - \sqrt{\left(\sigma_0 \sin\phi\right)^2 - \left(\tau_0 \cos\phi\right)^2}}{\cos^2\phi} \tag{34}
$$

$$\psi_0 = \frac{\pi}{2} + 0.5\left[\beta - \delta - \sin^{-1}\left(\frac{\sin(\delta+\beta)}{\sin\phi}\right)\right] \tag{35}$$

If $\psi_f \geq \psi_0$, no discontinuity exists in the stress filed and p_f can be found from Eq. (16) as

$$p_f = p_0 \exp\left[-2\tan\phi\left(\psi_f - \psi_0\right)\right], \qquad \psi_f \geq \psi_0 \tag{36}$$

and for $\psi_f \geq \psi_0$, p_f can be found from Eq. (19) as

$$p_f = p_0 \frac{\sin 2(\psi_0 - \omega_0)}{\sin 2(\psi_f - \omega_0)} \tag{37}$$

where from Eq. (18)

$$\omega_0 = 0.5\left[\psi_f + \psi_0 - \cos^{-1}\left(\sin\varphi\cos\left(\psi_f - \psi_0\right)\right)\right] \tag{38}$$

Finally the results for k_{aq} can be written as Eq. (25) where for $\psi_f \geq \psi_0$

$$A_q = \exp\left(-2\left(\psi_f - \psi_0\right)\tan\phi\right)\times \frac{(1-k_v)\left[\cos(\delta+\beta) - \sqrt{\sin(\phi-\delta-\beta)\sin(\phi+\delta+\beta)}\right]\cos\beta}{\cos^2\phi\cos\delta}, \quad \psi_f \geq \psi_0 \tag{39}$$

and for $\psi_f \geq \psi_0$

$$A_q = \frac{\sin 2(\psi_0 - \omega_0)}{\sin 2(\psi_f - \omega_0)}\times \frac{(1-k_v)\left[\cos(\delta+\beta) - \sqrt{\sin(\phi-\delta-\beta)\sin(\phi+\delta+\beta)}\right]\cos\beta}{\cos^2\phi\cos\delta}, \quad \psi_f < \psi_0 \tag{40}$$

k_{aq} can be found easily using Eqs. (25), (33), (35), (39) and (40). The computation can be done either by hand calculation or by using the MS Excel.

Solution for k_{ac}

A similar procedure can be used to compute k_{ac}. In this case, $q = \gamma = 0$ and

$$k_{ac} = \frac{p_a}{cH} = \frac{\sqrt{{\sigma_f}^2 + {\tau_f}^2}}{c\cos\theta} \tag{41}$$

The boundary conditions on the ground surface are

$$p_0 = c\frac{\sin\phi - 1}{\cos\phi} \tag{42}$$

$$\psi_0 = \frac{\pi}{2} + \beta \tag{43}$$

From Eqs. (16) and (19), p_f can be written as

$$\begin{aligned} p_f &= A_c c \\ A_c &= -\cot\phi + \left(\frac{1-\sin\phi}{\sin\phi\cos\phi}\right)\exp\left(-2\left(\psi_f - \psi_0\right)\tan\phi\right), \quad \psi_f \geq \psi_0 \\ A_c &= \left(\frac{\frac{1-\sin\phi}{\cos\phi}\sin 2\left(\psi_0 - \omega_0\right) - \cos\phi\sin 2\left(\psi_f - \omega_0\right)}{\sin\phi\sin 2\left(\psi_f - \omega_0\right)}\right), \quad \psi_f < \psi_0 \end{aligned} \tag{44}$$

where ω_0 can be found from Eq. (38). ψ_f can be written as (Eq. (15))

$$\psi_f = \frac{\pi}{2} + \theta + 0.5\left[-\delta_w + \sin^{-1}\left(\frac{\mathrm{A}_c\sin\delta_w + \lambda\cos\delta_w}{\mathrm{A}_c\sin\phi + \cos\delta_w}\right)\right] \tag{45}$$

where $\lambda = c_w / c$.

The lateral earth pressure coefficient k_{ac} can be computed from Eq. (26), using the parameters defined in Eqs. (43), (44) and (45). Eq. (45) is a nonlinear equation for ψ_f. This equation can be solved using the Solver tool in the MS Excel.